

# Synthesis, Molecular Editing, and Biological Assessment of the Potent Cytotoxin Leiodermatolide

Damien Mailhol,<sup>†</sup> Jens Willwacher,<sup>†</sup> Nina Kausch-Busies,<sup>†</sup> Elizabeth E. Rubitski,<sup>‡</sup> Zhanna Sobol,<sup>‡</sup> Maik Schuler,<sup>‡</sup> My-Hanh Lam,<sup>§</sup> Sylvia Musto,<sup>§</sup> Frank Loganzo,<sup>§</sup> Andreas Maderna,<sup>||</sup> and Alois Fürstner<sup>\*†</sup>

<sup>†</sup>Max-Planck-Institut für Kohlenforschung, D-45470 Mülheim/Ruhr, Germany

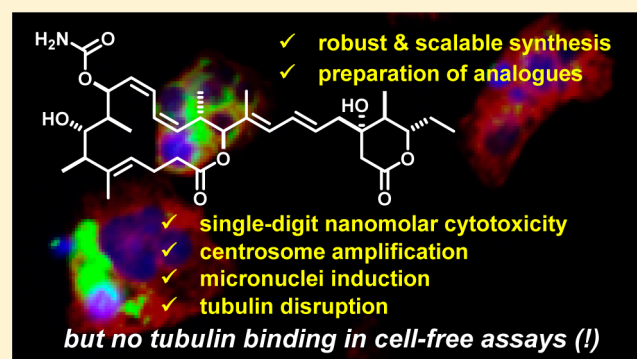
<sup>‡</sup>Pfizer Drug Safety Research and Development, 445 Eastern Point Road, Groton, Connecticut 06340, United States

<sup>§</sup>Pfizer Oncology, 401 North Middletown Road, Pearl River, New York 10965, United States

<sup>||</sup>Pfizer Oncology Medicinal Chemistry, 445 Eastern Point Road, Groton, Connecticut 06340, United States

## Supporting Information

**ABSTRACT:** It was by way of total synthesis that the issues concerning the stereostructure of leiodermatolide (**1**) have recently been solved; with the target now being unambiguously defined, the mission of synthesis changes as to secure a meaningful supply of this exceedingly scarce natural product derived from a deep-sea sponge. To this end, a scalable route of 19 steps (longest linear sequence) has been developed, which features a catalytic asymmetric propargylation of a highly enolizable  $\beta$ -keto-lactone, a ring closing alkyne metathesis and a modified Stille coupling as the key transformations. Deliberate digression from this robust blueprint brought a first set of analogues into reach, which allowed the lead qualities of **1** to be assessed. The acquired biodata show that **1** is a potent cytotoxin in human tumor cell proliferation assays, distinguished by  $GI_{50}$  values in the  $\leq 3$  nM range even for cell lines expressing the Pgp efflux transporter. Studies with human U2OS cells revealed that **1** causes mitotic arrest, micronucleus induction, centrosome amplification and tubulin disruption, even though no evidence for direct tubulin binding has been found in cell-free assays; moreover, the compound does not seem to act through kinase inhibition. Indirect evidence points at centrosome declustering as a possible mechanism of action, which provides a potentially rewarding outlook in that centrosome declustering agents hold promise of being inherently selective for malignant over healthy human tissue.



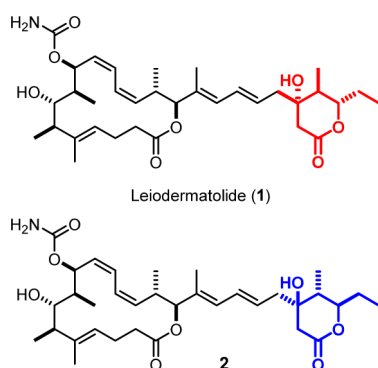
Bioassay-guided fractionation of the crude extracts of a lithistid *Leiodermatum* sponge collected by submersible in deep waters off the Florida coastline led to the isolation of leiodermatolide (**1**).<sup>1</sup> This macrolide is peculiar in that it was found to elicit abnormal spindle formation in two different cancer cell lines in the nM range although purified tubulin remained unaffected even at 20  $\mu$ M concentration.<sup>1</sup> These preliminary data have to be seen in the light of what is known about other antimitotic agents, which continue to represent the mainstay of systemic cancer chemotherapy. All clinically approved drugs of this functional type bind to tubulin as the primary target and, in doing so, disrupt the dynamics of microtubule assembly/disassembly in one way or the other.<sup>2–4</sup> Leiodermatolide (**1**) might be distinct in its mode of action and therefore merits closer scrutiny, in particular as it exhibited impressive antiproliferative activity against a small panel of human and murine cancer cell lines.<sup>1</sup>

Importantly, however, the isolated sample did not allow the structure of the compound to be firmly established. Even though advanced NMR spectroscopic techniques were masterfully used in combination with molecular modeling and

computational NMR prediction, only the relative configuration of the macrolide sector and of the  $\delta$ -lactone could be unraveled.<sup>1</sup> The pentadienyl spacer rendered it impossible to correlate these segregated stereoclusters with each other by spectroscopic means; likewise, the absolute configuration of leiodermatolide remained unknown.<sup>1</sup>

Our group was recently able to clarify both aspects.<sup>5</sup> To this end, compounds **1** and **2** were prepared which comprise the same macrolide core but feature two antipodal  $\delta$ -lactone segments (color coded). The NMR spectra of these two conceivable representations of leiodermatolide, recorded at 600 MHz, are in fact almost indistinguishable. Yet, based on very subtle differences in a subsector of the aliphatic region (2.20–2.50 ppm), we felt confident to assign the relative stereostructure of leiodermatolide as shown in **1**; the absolute configuration was inferred from the optical rotation data.<sup>5</sup> A later independent synthesis by the Paterson group confirmed our conclusions.<sup>6,7</sup>

Received: August 27, 2014



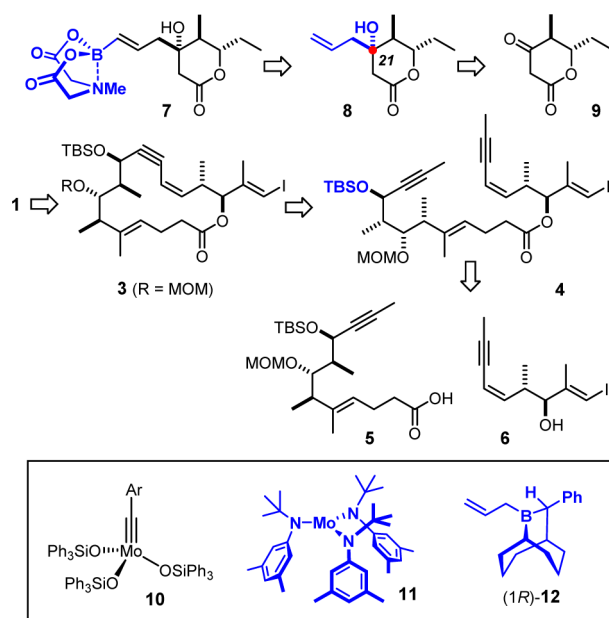
The unusually subtle spectral differences between leiodermatolide (1) and its diastereomer 2 rendered total synthesis indispensable for the structure elucidation.<sup>5</sup> Synthesis, however, finds an even more important mission in procuring a meaningful quantity of this unorthodox antimetabolic agent derived from a deep-sea organism, which, even if it were accessible, might not be a reliable source.<sup>8</sup> With this in mind,<sup>9</sup> we embarked onto a second generation synthesis of 1 that should be robust, productive, scalable and flexible. The results of this venture and of a first round of biological assessment of leiodermatolide and a set of congeners are summarized below.

## RESULTS AND DISCUSSION

**Strategic Considerations.** In our original approach, 1 had been dissected into the three major fragments 5, 6 and 7, which allowed the target to be assembled by esterification, cross coupling and ring closing alkyne metathesis (RCAM) (Scheme 1).<sup>5</sup> We sought to retain this blueprint, not least for its inherent flexibility. Moreover, the access routes to segments 5 and 6 and their fusion to diene 4 were deemed quite satisfactory and should qualify, with only minor modifications, for higher material throughput.

However, the following issues needed to be revisited:

### Scheme 1. First-Generation Synthesis of 1<sup>a</sup>



<sup>a</sup>The major issues to be addressed in a revised synthesis are color-coded.

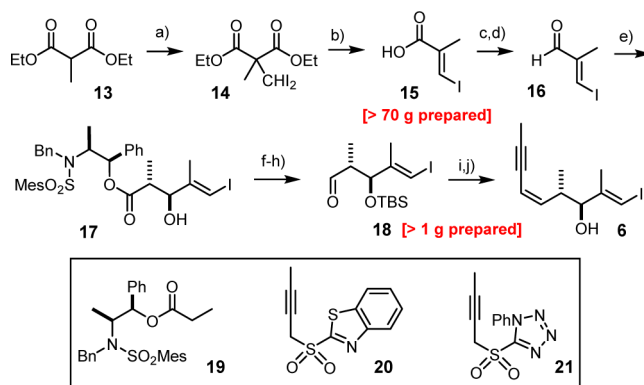
(1) The fragment coupling by a Suzuki reaction<sup>10</sup> between the MIDA-boronate ester 7 and iodide 3 proved unusually challenging. Only the use of Tl(OEt) in aqueous THF led to reasonable results,<sup>11</sup> but engendered partial saponification of the  $\delta$ -lactone. Although an acidic workup allowed this problem to be remedied, the conditions must be carefully controlled not to endanger the acid sensitive protecting groups and the isomerization-prone unsaturations on the backbone. With an overall yield of no more than 55%, this seemingly routine step was the bottleneck of our first approach to 1. A more robust solution had to be found, that should also make the use of a thallium base obsolete.

(2) The carbon spacer between the macrolide and the  $\delta$ -lactone is *axially* disposed at C.21. This conspicuous connectivity pattern had been set by a reagent controlled allylation of the cyclic  $\beta$ -ketoester 9 with allyl borane (*R*)-12;<sup>12</sup> although quite efficient, the preparation of this elaborate reagent requires diazoalkane chemistry and fractional crystallization.<sup>13</sup> It is obvious that a catalytic alternative would render a scale up exercise much more practical.

(3) Ring closure of diene 4 to the macrolactone core 3 by RCAM<sup>14,15</sup> worked well but mandated the use of the very sensitive precatalyst 11.<sup>16</sup> The unexpected failure of the usually superior molybdenum alkylidyne 10 in this particular case was tentatively ascribed to steric factors.<sup>17,18</sup> This aspect warranted closer inspection, if not for the sake of material supply then at least for a better understanding of alkyne metathesis in general.

**The Enyne Segment.** As expected, minor modifications sufficed to adjust the original route to the enyne fragment 6 to the current needs (Scheme 2). The initial alkylation of 13 with

### Scheme 2. Preparation of the Enyne Fragment<sup>a</sup>



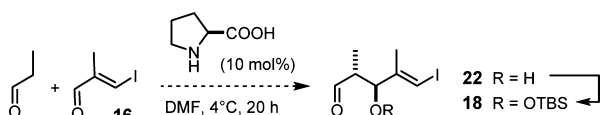
<sup>a</sup>Reagents and conditions: (a)  $\text{CHI}_3$ , NaH,  $\text{Et}_2\text{O}$ , reflux, 99%; (b) KOH,  $\text{EtOH}/\text{H}_2\text{O}$ , reflux, 91%; (c)  $\text{BH}_3(\text{THF})$ , THF,  $-30^\circ\text{C} \rightarrow \text{RT}$ ; (d) air,  $[\text{Cu}(\text{MeCN})_4]\text{OTf}$  (5 mol %), bipyridine (5 mol %), TEMPO (5 mol %), *N*-methylimidazole (10 mol %), MeCN, 55% (over both steps); (e) 19,  $\text{Cy}_2\text{BOTf}$ ,  $\text{Et}_3\text{N}$ ,  $\text{CH}_2\text{Cl}_2$ ,  $-78^\circ\text{C} \rightarrow \text{RT}$ , 76%; (f) TBSOTf, 2,6-dimethyl-pyridine,  $\text{CH}_2\text{Cl}_2$ ,  $-10^\circ\text{C}$ ; (g) DIBAL-H, toluene,  $-78^\circ\text{C}$ , 83% (over both steps); (h) Dess–Martin periodinane,  $\text{CH}_2\text{Cl}_2$ ,  $0^\circ\text{C}$ , 96%; (i) 20, KHMDS, THF,  $-55^\circ\text{C}$ , 51% (*Z*:*E* > 20:1) (over both steps); (j) TBAF, THF,  $0^\circ\text{C}$ , 98%.

$\text{CHI}_3$  and the subsequent Krapcho decarboxylation worked admirably well on massive scale. In contrast, it was advantageous to replace  $\text{LiAlH}_4$  as the reducing agent for acid 15 by  $\text{BH}_3\cdot\text{THF}$ ; the crude product was then directly engaged in a copper/TEMPO cocatalyzed air oxidation<sup>19</sup> to furnish the known aldehyde 16,<sup>20</sup> which was clearly more practical than the use of overstoichiometric  $\text{MnO}_2$  that we had originally chosen.<sup>5</sup>

Freshly prepared **16** was subjected to a Masamune–Abiko *anti*-aldol reaction,<sup>21</sup> which allowed multigram quantities of diastomerically pure **17** to be secured. This compound was transformed into aldehyde **18** on demand, which was immediately used for a Julia reaction with sulfone **20**<sup>22,23</sup> to furnish enyne **6** with impeccable *Z*-selectivity ( $\geq 20:1$ ); the analogous tetrazolyl-sulfone **21** gave lower yields ( $\leq 42\%$ ).

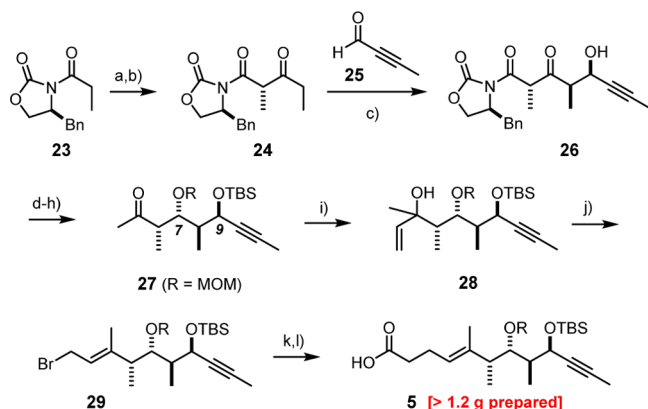
Attempts to prepare aldehyde **18** more directly by means of a proline-catalyzed *anti*-aldol reaction were unsuccessful (Scheme 3);<sup>24</sup> only self-condensation of propanal as the necessary partner was observed, whereas **16** was basically not engaged. Therefore, this seemingly lucrative shortcut was abandoned.

### Scheme 3. Attempted Shortcut



**The Acid Segment.** Good amounts of the carboxylic acid fragment **5** were secured by adaptation of our original approach (Scheme 4).<sup>5</sup> In brief, the sequence benefits from the

### Scheme 4. Preparation of the Acid Segment<sup>a</sup>



<sup>a</sup>Reagents and conditions: (a)  $\text{Bu}_2\text{BOTf}$ ,  $\text{Et}_3\text{N}$ , propanal, 98%; (b)  $\text{SO}_3$ -pyridine,  $\text{CH}_2\text{Cl}_2$ , DMSO,  $\text{Et}_3\text{N}$ ,  $-15^\circ\text{C}$ , 75%; (c) **25** (5 equiv),  $\text{Sn}(\text{OTf})_2$ ,  $\text{Et}_3\text{N}$ ,  $\text{CH}_2\text{Cl}_2$ ,  $-20^\circ\text{C}$ , 83% (dr = 9:1); (d)  $\text{Me}_4\text{NBH}(\text{OAc})_3$ , HOAc, MeCN,  $-50^\circ\text{C}$ , 95% (dr = 92:8); (e) TBSOTf,  $\text{Et}_3\text{N}$ ,  $\text{CH}_2\text{Cl}_2$ ,  $-78^\circ\text{C} \rightarrow 0^\circ\text{C}$ , 89%; (f)  $(\text{MeO})\text{NHMe}\cdot\text{HCl}$ ,  $\text{AlMe}_3$ , THF,  $0^\circ\text{C} \rightarrow \text{RT}$ , 92%; (g) MOMCl,  $(i\text{Pr})_2\text{NEt}$ , DMF,  $50^\circ\text{C}$ , 98%; (h)  $\text{MeMgCl}$ ,  $\text{Et}_2\text{O}$ ,  $0^\circ\text{C}$ , 98%; (i)  $\text{CH}_2=\text{CHMgCl}$ , THF,  $-78^\circ\text{C} \rightarrow \text{RT}$ , 92%; (j)  $\text{PBr}_3$ , pyridine,  $\text{Et}_2\text{O}$ ,  $0^\circ\text{C}$ , 83%; (k) EtOAc, LDA, CuI, THF,  $-110^\circ\text{C} \rightarrow -30^\circ\text{C}$ , 58%; (l)  $\text{Me}_3\text{SiOK}$ ,  $\text{Et}_2\text{O}$ , 98%.

robustness of the Evans aldol reaction of **24** with an excess of **25**,<sup>25</sup> for optimal results, it is essential that the  $\text{Sn}(\text{OTf})_2$  promoter is rigorously acid free. The  $\text{MnO}_2$  oxidation originally used to prepare aldehyde **25** was replaced by a more practical TEMPO-catalyzed, NCS-mediated oxidation of commercial 2-butynol in buffered medium.<sup>26</sup> A subsequent 1,3-*anti*-reduction<sup>27</sup> of **26** preceded the elaboration of the auxiliary terminus into the corresponding methyl ketone **27**; interwoven was the regioselective silylation of the propargylic alcohol and the orthogonal MOM-protection of the remaining hydroxyl group to ensure a selective installation of the signature carbamate of leiodermatolide later in the synthesis.<sup>28,29</sup>

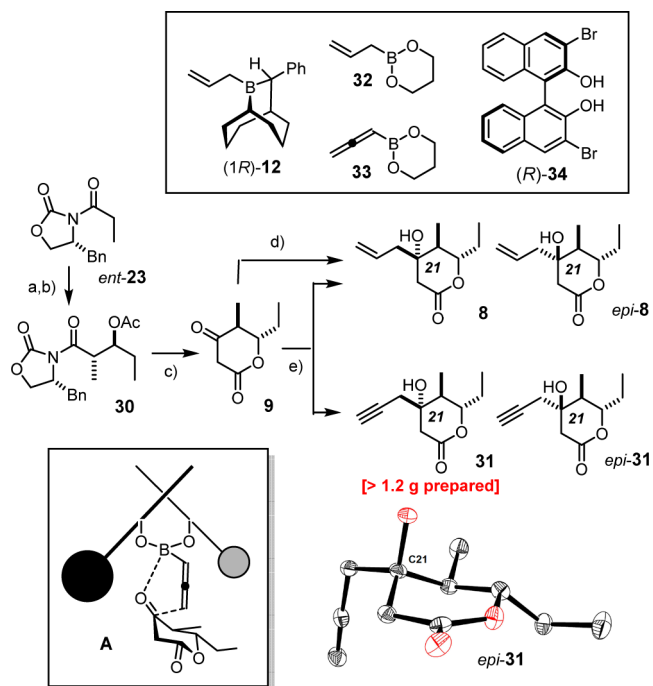
Addition of vinylmagnesium bromide to **27** followed by bromination of the resulting allylic alcohol **28** in an  $\text{S}_{\text{N}}2'$  mode

set the stage for a chain extension by alkylation with the lithium enolate of ethyl acetate in the presence of CuI.<sup>30</sup> Saponification of the resulting ester with TMSOK furnished the required acid segment **5** without incident.

**Scalable Synthesis of the  $\delta$ -Lactone Segment.** As mentioned above, a subtle but distinctive structural attribute of leiodermatolide (**1**) is the axial disposition of the carbon branch on the  $\delta$ -lactone at C.21. It had been cautiously questioned in the past whether this stereochemical peculiarity was a misassignment of the isolation team;<sup>7c</sup> however, the first generation syntheses of **1** unambiguously confirmed this salient connectivity pattern.<sup>5</sup>

Our original approach to the required building block hinged upon a reagent-controlled allylation of the cyclic  $\beta$ -ketoester **9**, which is accessible on multigram scale by an Evans *anti*-aldol reaction followed by an intramolecular Claisen condensation of the derived acetate **30** (Scheme 5).<sup>5,31</sup> The crucial allylation,

### Scheme 5. Synthesis of the $\delta$ -Lactone Segment<sup>a,b</sup>



<sup>a</sup>Reagents and conditions: (a)  $\text{Bu}_2\text{BOTf}$  (2 equiv),  $\text{Et}_3\text{N}$ , propanal,  $\text{Et}_2\text{O}$ ,  $-78^\circ\text{C}$ , 74% (dr = 11:1); (b)  $\text{Ac}_2\text{O}$ ,  $\text{Et}_3\text{N}$ , DMAP cat.,  $\text{CH}_2\text{Cl}_2$ ,  $0^\circ\text{C}$ , 82%; (c) LiHMDS, THF,  $-78^\circ\text{C}$ , 83%; (d) (1*R*)-**12** (1.1 equiv), 86% (dr = 5.5:1); (e) see Table 1. <sup>b</sup>The inset shows the solid state structure of the minor isomer *epi*-**31** with an equatorially disposed propargyl branch.

however, worked only after two significant challenges had been overcome: first, **9** is highly enolizable and attempted reactions with a host of allylmethyl reagents led to marginal conversions, if any. Only an allylindium reagent generated in situ as well as 9-allyl-9-BBN resulted in good conversions, but delivered the wrong isomer *epi*-**8** as the major product.

To override this inherent bias, we resorted to borane **12** as a powerful chiral variant of 9-allyl-9-BBN.<sup>13</sup> In fact, treatment of **9** with (1*R*)-**12** furnished the desired product **8** with an appreciable selectivity (dr = 5.5:1).<sup>12</sup> A subsequent cross metathesis of **8** gave MIDA-boronate **7**<sup>32</sup> (Scheme 1) in readiness for Suzuki coupling with the macrocyclic alkenyl iodide **3** as an adequate electrophilic counterpart.

Though ultimately successful,<sup>5</sup> we saw the need to amend this strategy. First, a catalytic substitute for the stoichiometric allyl-donor **12** was desirable, as was a better solution for the problematic cross coupling step (see above). We conjectured that binaphthol-derived allylboronates exhibit similar chemical characteristics as **12** and might therefore provide a window of opportunity. Such reagents had originally been used in stoichiometric amounts,<sup>33</sup> but Schaus and co-workers later showed that the combination of **32** with catalytic amounts of a 3,3'-disubstituted 2,2'-binaphthol derivative such as **34** is effective; under these conditions, a host of ketones were allylated with generally excellent levels of selectivity.<sup>34</sup> A single application to an acyclic  $\beta$ -ketoester made us confident that this method might be applicable in the present context.

In fact, reaction of **9** with boronate **32** in toluene in the presence of **34** (10 mol %) and *tert*-BuOH (2 equiv) at ambient temperature furnished the desired product **8** with an encouraging selectivity (dr = 4:1), but the conversion was low and erratic (ca. 15–40% after 19 h) (Scheme 1) (Table 1,

**Table 1. Catalytic Asymmetric Allylation or Propargylation of  $\beta$ -Ketolactone **9**<sup>a</sup>**

entry	reagent	catalyst	yield (%)	<b>8</b> ( <b>31</b> ): <i>epi</i>
1	<b>32</b>	<i>R</i> - <b>34</b>	15–40 <sup>b,c,d</sup>	4:1
2	<b>32</b>	<i>R</i> - <b>34</b>	84 <sup>d</sup>	6.2:1
3	<b>32</b>	<i>R</i> - <b>34</b>	95	6.1:1
4	<b>32</b>	<i>S</i> - <b>34</b>	88 <sup>d</sup>	1:9.0
5	<b>33</b>	<i>R</i> - <b>34</b>	94	7.6:1
6	<b>33</b>	<i>R</i> - <b>34</b> <sup>c</sup>	80	6.6:1
7	<b>33</b>	<i>S</i> - <b>34</b>	87	1:15

<sup>a</sup>Unless stated otherwise, all reactions were performed with **34** (10 mol %) in toluene at 130 °C under microwave heating. <sup>b</sup>Conversions (GC). <sup>c</sup>At ambient temperature without microwave heating. <sup>d</sup>In the presence of *t*BuOH (2 equiv). <sup>e</sup>Using only 2 mol % of **34**.

entry 1). Deviation from these original literature conditions allowed the problem to be fixed: thus, the addition of *tert*-BuOH was found unnecessary (cf. entries 2/3) and microwave irradiation dramatically accelerated the conversion without diminishing the diastereoselectivity; actually, the dr in favor of the desired isomer **8** was slightly improved despite the high reaction temperature. Moreover, the comparison with entry 4 shows that the addition is catalyst-controlled. Overall, this operationally simple method compares favorably with the use of the much more elaborate allylborane **12** as a stoichiometric allyl donor in this particular case.

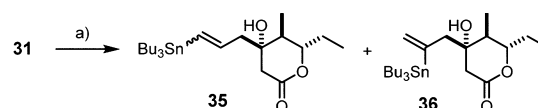
Propargylation of **9** could be achieved analogously upon replacement of **32** by allenylboronate **33** (Table 1, entries 5–7).<sup>35</sup> This reaction provided an even better outcome, although attempts at lowering the catalyst loading led to a slight erosion in yield and selectivity. To the best of our knowledge, this is the first catalytic propargylation of a highly enolizable substrate.<sup>36</sup> The stereochemical course was ascertained by X-ray diffraction, which proved that the *minor* isomer *epi*-**31** features an equatorially oriented propargyl substituent (see insert in Scheme 5). The favored axial delivery of the nucleophile can be rationalized by a transition state of type **A**, which assumes that the cyclic boronate **33** undergoes full exchange with the chiral diol catalyst as originally proposed by Goodman.<sup>37</sup> Under this premise, *tert*-BuOH should not play an immediate role in the selectivity-determining step, which is in accord with our data. The substrate then immerses into the tight cleft formed by

the 3,3'-dibromo-2,2'-binaphthol scaffold such that the bulky substituents point toward the open quadrant in the back. In any case, this convenient methodology allowed gram amounts of **8** and **31** to be secured.

Previous experiences had taught us that modified Stille reactions often outperform the Suzuki cross coupling when dealing with polyunsaturated and/or base-sensitive compounds.<sup>38,39</sup> Since the late-stage fragment coupling of iodide **3** with boronate **7** in our original approach to **1** was far from optimal,<sup>5</sup> it seemed reasonable to replace **7** by the corresponding stannane **35** as a potentially more adequate donor.

Hydrostannation of **31** should provide access to this reagent (Scheme 6).<sup>40</sup> Under free radical conditions, however, the

**Scheme 6. Preparation of the Stannane Donor<sup>a</sup>**

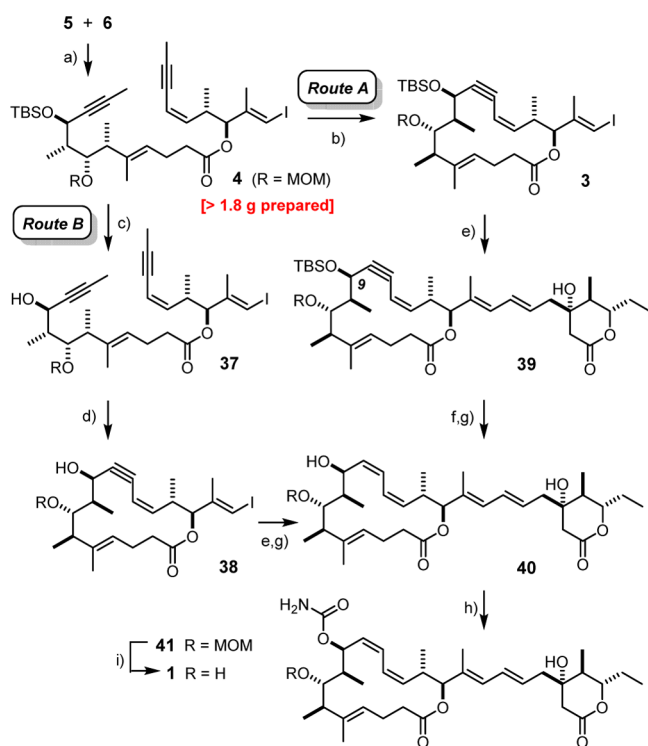


<sup>a</sup>Reagents and conditions: (a) Bu<sub>3</sub>SnH (over 15 min), Pd<sub>2</sub>(dba)<sub>3</sub> (1 mol %), PCy<sub>3</sub>·HBF<sub>4</sub> (4 mol %), *i*PrNEt<sub>2</sub> (8 mol %), CH<sub>2</sub>Cl<sub>2</sub>, *E*-**35** (72%) and **36** (15%).

terminal stannane **35** was obtained in low yield as a futile *E/Z*-mixture, whereas recourse to standard palladium catalysts afforded substantial amounts of the internal alkenyl tin derivative **36** in addition to product *E*-**35**. After some optimization it was found that stannane *E*-**35** could be procured in good yield as a single geometrical isomer with the aid of a catalyst formed in situ from Pd<sub>2</sub>(dba)<sub>3</sub> and PCy<sub>3</sub>,<sup>41</sup> provided that Bu<sub>3</sub>SnH was added slowly to ensure complete conversion of the substrate; small amounts of isomer **36** formed under these conditions were removed by flash chromatography. As will be outlined below, this optimization paid valuable dividends because the late-stage Stille reaction with iodide **3** proved in fact to be robust and exquisitely productive.

**Macrocyclization and Completion of the Total Synthesis.** With reliable routes to all building blocks in place, we turned our attention to the optimization of the fragment coupling steps and the completion of the total synthesis. As expected, the esterification of **5** and **6** proved uneventful. The subsequent macrocyclization of diyne **4** also worked well with complex **11** as precatalyst, which is activated in situ on treatment with CH<sub>2</sub>Cl<sub>2</sub> as previously described by our group (Scheme 7, route A).<sup>16</sup> In contrast, the alkylidyne complex **10**<sup>17</sup> endowed with more bulky triphenylsilylanolate ligands only led to the formation of an acyclic dimer via metathesis at the sterically less hindered enyne-triple bond of the substrate (for the catalysts, see Scheme 1).

Although the cyclization of **4** with the help of **11**/CH<sub>2</sub>Cl<sub>2</sub> was productive, fairly harsh conditions and a long reaction time were necessary; these factors, in turn, may account for the necessary high catalyst loading. The obvious difficulty in closing the macrocyclic ring of **3** can be ascribed to (i) steric hindrance of the propargylic triple bond in **4** exerted by the neighboring TBS-ether, (ii) an electronic handicap of the conjugated enyne subunit, and/or (iii) the ring strain caused by the three sites of unsaturation within the 16-membered frame (see below). Nevertheless, the chemoselectivity of the reaction is remarkable in that the catalyst rigorously distinguished between the

Scheme 7. Completion of the Total Synthesis<sup>a</sup>

<sup>a</sup>Reagents and conditions: (a) EDCI-HCl, DMAP, CH<sub>2</sub>Cl<sub>2</sub>, 0 °C, 96%; (b) **11** (40 mol %), CH<sub>2</sub>Cl<sub>2</sub>/toluene, 100 °C, 72%; (c) TBAF, THF, 4 Å MS, 0 °C, 88%; (d) **10** (15 mol %), toluene, RT, 61%; (e) **35**, Pd(PPh<sub>3</sub>)<sub>4</sub> (5 mol %), CuTC, [Ph<sub>2</sub>PO<sub>2</sub>][NBu<sub>4</sub>], DMF, 93% (from **3**), 90% (from **38**); (f) TBAF, THF, 4 Å MS, 0 °C, 81%; (g) Zn(Cu/Ag), THF/H<sub>2</sub>O/MeOH, 50 °C, 92%; (h) Cl<sub>3</sub>CC(O)NCO, CH<sub>2</sub>Cl<sub>2</sub>, -78 °C, then Al<sub>2</sub>O<sub>3</sub>, 75%; (i) Me<sub>2</sub>BBr, CH<sub>2</sub>Cl<sub>2</sub>, -90 °C → -78 °C, 86%.

different  $\pi$ -systems presented by the cyclization precursor and did not damage the reactive alkenyl iodide either.<sup>42</sup>

The presence of this particular functional group in **3** defined the order of the subsequent steps. To avoid any issues with potential deiodination, cross coupling of **3** with the  $\delta$ -lactone segment has to precede the semireduction of the cycloalkyne unit.<sup>43</sup> As mentioned above, a Suzuki reaction with boronate **7** had provided only a modest 55% yield, despite considerable optimization.<sup>5</sup> It was therefore gratifying to see that the analogous Stille reaction with stannane **35** furnished the desired product **39** in well reproducible 93% yield. This significant improvement was made possible by a protocol that relies on the combined use of Pd(PPh<sub>3</sub>)<sub>4</sub>, CuTC and [(*n*Bu<sub>4</sub>N)(Ph<sub>2</sub>PO<sub>2</sub>)] in DMF at ambient temperature. These essentially neutral and fluoride free conditions had been developed for applications to particularly sensitive and/or silyl-bearing substrates.<sup>44–46</sup> These conditions also ensure exceptionally high rates; in the present case, the coupling was quenched after 1 min (!) reaction time, thus minimizing exposure of the sensitive materials to the reagents.

In marked contrast to the ease of this modified fragment coupling, the alkyne subunit in product **39** failed to undergo semireduction under a variety of conditions. This critical transformation could only be accomplished after the TBS-group at the neighboring C.9–OH site had been removed. Treatment of the resulting alcohol derivative with Zn(Cu/Ag) couple in protic medium<sup>47</sup> resulted in clean formation of

product **40** as a single geometrical isomer. This favorable outcome corroborates the notion that alkyne metathesis is particularly relevant for the preparation of polyunsaturated targets.<sup>48</sup> This includes nonthermodynamic *Z,Z*-configured motifs as present in **1**, which currently remain difficult, if not impossible, to prepare by metathesis otherwise.<sup>49</sup>

The fact that the semireduction would not proceed in the presence of a flanking silyl ether lent credence to the notion that the difficulties in the metathetic ring closure might equally be caused by steric hindrance of the propargylic site of diyne **4**. To probe this aspect, the inflicting TBS-group was cleaved and the resulting product **37** engaged in RCAM (Scheme 7, route B). This amendment brought the molybdenum alkylidyne **10** back on stage,<sup>17,50</sup> which had failed with **4** but allowed the slimmer compound **37** to be cyclized without incident to the corresponding cycloalkyne **38** even at ambient temperature. From the chemical viewpoint, this outcome is deemed remarkable if one considers that Schrock alkylidynes are inherently nucleophilic at the  $\alpha$ -carbon atom and therefore sensitive to protic sites.<sup>51</sup> The compatibility of **10** with unprotected –OH groups is largely unprecedented; this quality augurs well for future applications of alkyne metathesis to chemically demanding cases.<sup>52</sup> Product **38** was then engaged in a Stille cross coupling with **35**, thus intercepting the route outlined above.

At this stage, the yet missing carbamate moiety was introduced by treatment of **40** with Cl<sub>3</sub>CC(O)NCO followed by mild hydrolysis of the primary adduct on treatment with alumina.<sup>53</sup> The final MOM-cleavage originally faced significant problems, although a variety of reagents were screened.<sup>28</sup> Gratifyingly, Me<sub>2</sub>BBr proved uniquely suited for this delicate transformation;<sup>54</sup> this reagent did not damage the sensitive allylic carbamate, the tertiary alcohol functions or any of the potentially isomerization-prone olefinic sites.

Leiodermatolide (**1**) was thus procured in 6% overall yield over the 19 steps of the longest linear sequence. Importantly, all supply limiting transformations of the first generation synthesis have been replaced by robust alternatives; in this context, the catalytic asymmetric propargylation of the enolizable  $\beta$ -keto-lactone **9** and the Stille coupling in lieu of the Suzuki reaction denote particularly substantial improvements. Equally noteworthy is the fact that two solutions for the RCAM step were found once it had been recognized that the original difficulties in closing the macrocyclic frame were steric in origin. The new route allows gram quantities of all building blocks to be made without undue efforts. If elaborated as described above, substantial amounts of the natural product come into reach. Yet, we abstained from funneling all material available to us into this route and made only 50 mg of **1** in the first place (with all conditions optimized, the produced 1.8 g of **4** would afford ca. 500 mg of **1**). This decision was based on safety consideration in view of the significant cytotoxicity of this compound (see below), as well as on the wish to use the advanced intermediates as a platform for a first round of diverted total synthesis.<sup>55</sup> Yet, it is clear that a reliable supply chain is now in place that certainly allows for a detailed evaluation of this otherwise extremely scarce deep-sea macrolide.

**Structural Considerations.** Leiodermatolide, as isolated from the sponge, was described as an amorphous white powder. With substantial amounts of synthetic material in hand, we managed to grow single crystals of a fortuitous monohydrate. Figure 1 depicts the structure of **1** in the solid state in two different orientations.

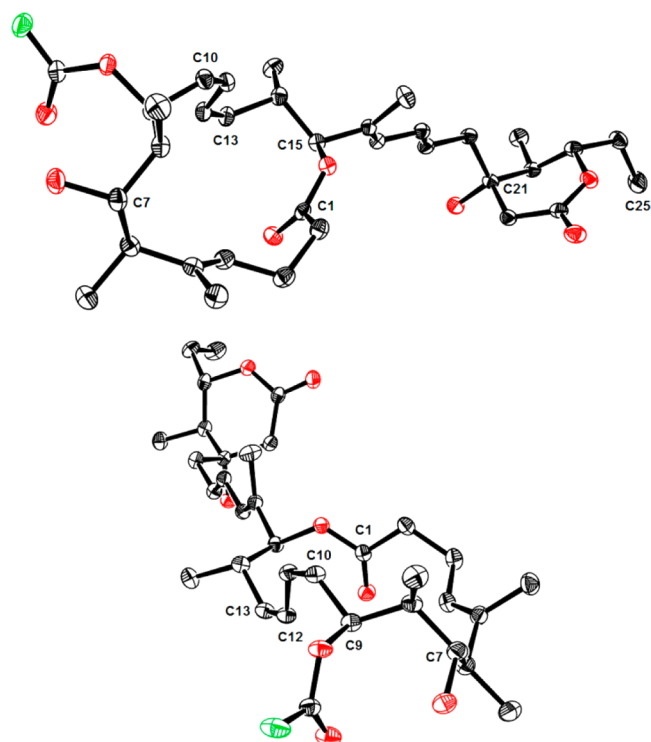


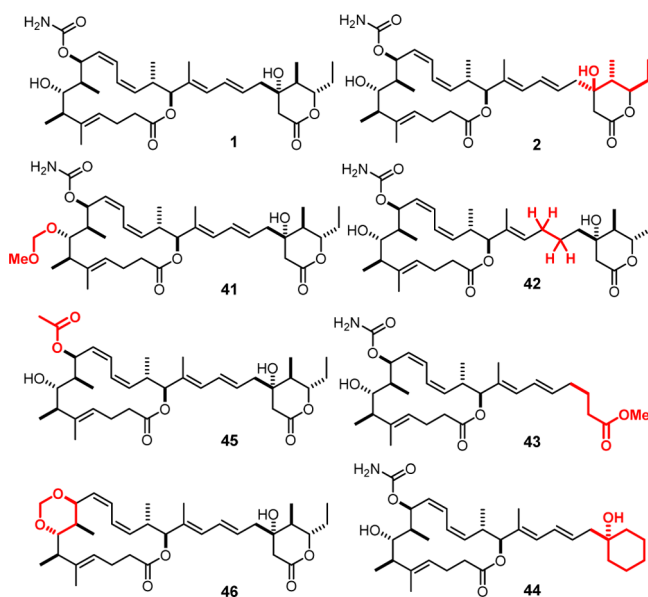
**Figure 1.** Structure of **1** in the solid state; the cocrystallized water molecule is omitted for clarity.

The top view shows the conspicuous axial attachment of the carbon branch on the  $\delta$ -lactone. Moreover, the extended coplanar conformation of the pentadienyl spacer is clearly visible that ensures optimal orbital overlap within the inscribed C.16-C.19 *s-trans* diene. This stiff array holds the six-membered ring at distance from the macrocycle. Since it had originally proven impossible to mutually correlate these substructures by spectroscopic means, it is likely that a similar arrangement is populated in solution.

The bottom view zooms in on the macrolide sector. As expected, the lactone carbonyl is axially oriented. The *Z,Z*-configured diene region (C.10-C.13) is tilted such that it stands almost perpendicular to the plane of the fairly puckered 16-membered ring.<sup>56</sup> The carbamate carbonyl atom and the C.7-OH likely engage in a stabilizing hydrogen bond. Although the proton of the bridge has not been localized in a difference Fourier map, the short distance between its calculated position and the carbonyl (2.116 Å) as well as the relative orientation of the two functionalities are suggestive. This notion is supported by a distinctive spectral signature: thus, the signals of the protons on the rim of the macrocycle of **41** show line broadening. When the MOM-group is cleaved and the C.7-OH set free, the corresponding signals become well resolved (see the Supporting Information). This observation is consistent with the assumed formation of a hydrogen bond between the released hydroxyl group and the neighboring carbamate that reduces the conformational freedom and may therefore be of functional relevance.

**Molecular Editing.** No information whatsoever as to the pharmacophore of leiodermatolide was available at the outset of this project. Therefore, we extended our program to the preparation of a small set of non-natural analogues (Chart 1). This diverted total synthesis exercise<sup>55</sup> might show whether **1** is

### Chart 1. Derivatives and Analogues for Testing<sup>a</sup>



<sup>a</sup>Structural modifications relative to **1** are color-coded.

a singularity or qualifies as a possible lead in the quest for cytotoxic agents with an unorthodox mode of action.

The approaches to the individual compounds follow the logic outlined above, even though the specific steps have not been optimized (for details see the Supporting Information). They comprise structural point mutations that reflect the acquired intelligence in the following ways:

(1) Compound **2** had originally been considered as the other possible candidate to represent leiodermatolide (see Introduction); it comprises the identical macrolide portion but differs from the natural product by the antipodal headgroup. While **1** and **2** are hardly distinguishable by spectroscopic means,<sup>5</sup> the comparison of their bioactivity will unravel any innate functional link between the segregated stereoclusters.

(2) In compound **42** one of the double bonds of the spacer has been edited out to reduce its stiffness.

(3) Compounds **43** and **44** comprise more drastic changes. Because our original synthesis of **1** had shown the  $\delta$ -lactone to be hydrolysis-prone, this entity was replaced by an arguably more labile ester on the one hand and by an inert cyclohexanol ring on the other hand.

(4) The tantalizing possibility that a hydrogen bond between the carbamate carbonyl and the C.7-OH group is structure determining and therefore also functionally relevant was probed in the following ways: compound **41** as the immediate precursor of **1** but with the MOM-acetal still in place was subjected to testing as a putative “negative” control; conversely, compound **45** was prepared which features an acetate instead of the carbamate as an only gradually less potent hydrogen bond acceptor; finally, product **46** seemed interesting for its six-membered cyclic acetal can be seen as a rigid covalent linker in lieu of the hydrogen bonding array in question.

**Cytotoxicity.** Leiodermatolide showed excellent potencies in tumor cell proliferation assays using a select panel of seven human cancer cell lines. The  $GI_{50}$ 's after 4 days incubation were 0.4–3 nM (Table 2); of particular note is the fact that this impressive potency was also observed for the HEL92.1.7 cell line that expresses the Pgp efflux transporter, which is a major cause of resistance of leukemias against cancer chemotherapy.

**Table 2. Effect of 1 on Cancer Cell Cytotoxicity<sup>a</sup>**

cell line	histotype	GI <sub>50</sub> (nM)
N87	gastric	2.4
MDA-MB-361-DYT2	breast	3.5
HT29	colon	2.5
HL60	leukemia	1.0
NB4	leukemia	0.4
HEL92.1.7	leukemia	1.0
Raji	leukemia	0.9

<sup>a</sup>After 4 days treatment; for details, see the Supporting Information.

This may be taken as an indication that **1** does not constitute an effective efflux substrate, although more detailed studies to confirm these preliminary findings are warranted.

Encouraged by these results, our set of analogues and synthetic intermediates was assayed. GI<sub>50</sub> values were determined for those compounds for which a first dosing screen had indicated appreciable activity <1 μM. In addition to leiodermatolide itself, five compounds passed this threshold (Table 3). The most potent of these is product **45** bearing an

**Table 3. Assessment of the Cytotoxicity (GI<sub>50</sub>, nM) of Analogues after 4 Days Treatment**

	HL60	NB4	HEL <sup>b</sup>	Raji	HT29	N87	361 <sup>a</sup>
<b>1</b>	1.0	0.4	1.0	0.9	2.5	2.4	3.5
<b>45</b>	13.0	17.5	1.4	67.9	5.9	8.0	>10
<b>42</b>	35.8	14.8	51.0	66.5	40.6	41.1	52.6
<b>41</b>	>100	>100	>100	>100	>100	50.4	44.6
<b>2</b>	nd	nd	nd	nd	199.3	144.9	306.5
<b>44</b>	nd	nd	nd	nd	480.2	288.6	422.3

<sup>a</sup>MDA-MB-361-DYT2 cell line; nd = not determined. <sup>b</sup>HEL92.1.7.

acetate moiety instead of the carbamate, followed by the dihydro derivative **42** comprising a single olefin instead of the 1,3-diene within the spacer, which still shows appreciable cytotoxicity. Not unexpectedly, **41** as the MOM-protected precursor to **1** is less potent. These data suggest that an intact hydrogen bond between the C.7-OH and an adjacent carbonyl is important for maximizing potency. The carbamate itself seems to be a permissive site, which might become relevant, for example, in the preparation of antibody-drug conjugates (ADC).<sup>57</sup> In line with this overall picture the rigidified compound **46** with a cyclic acetal on the backbone did not meet the 1 μM cutoff.

Of particular note is the fact that compound **2** comprising the antipodal δ-lactone is at least 2 orders of magnitude less potent than **1**, even though these two diastereomers are almost indistinguishable by NMR. This differential provides an unambiguous biological confirmation for our original structure assignment and reveals an intimate functional link between the two lactone subunits of **1**, albeit their interrelation is spectroscopically almost intangible.

Somewhat unexpectedly, analogue **44** with the cyclohexyl headgroup retains submicromolar activity, whereas **43** terminated by a simple methyl ester had already been sorted out during the prescreening. These findings suggest that the specific decoration of the δ-lactone in **1** is functionally relevant in that it likely imparts chemical stability. All other tested compounds showed no appreciable cytotoxicity below 1 μM.

**Biological Assessment.** High content image analysis techniques have been previously established to study tubulin

disruption and associated cellular damage end points in whole cells.<sup>58</sup> In the current study, these techniques were utilized to gain insight about the mechanism by which leiodermatolide (**1**) causes mitotic arrest (for details, see the Supporting Information). Human osteosarcoma-derived U2OS cells were treated with **1** and assessed for cell cycle distribution, micronucleus induction, centrosome enumeration and tubulin disruption.

Cell cycle distribution was assessed by measuring the total DNA content in DAPI-stained cells. Figure 2 depicts the

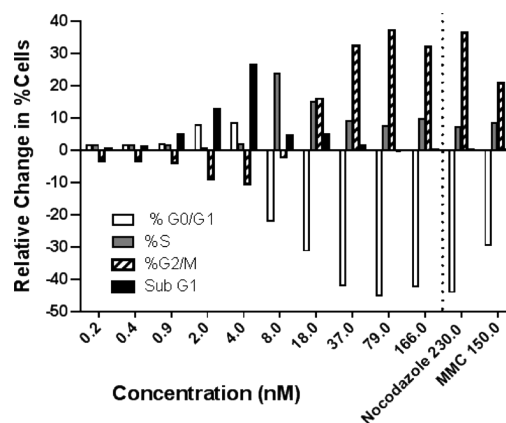


**Figure 2.** Cell cycle distribution relative to control: Relative increase in the %-cells distributed among cell cycle phases after exposure with **1** for 24 h.

change in cell cycle distribution of cultures treated with **1** as compared to the concurrent negative control. Accumulation of cells in G2/M began at 18 nM and continued to increase in a dose-dependent manner. A dose-dependent decrease in the G0/G1 cell population was seen starting at 8 nM, which is indicative of a decrease in the number of cycling cells. A subG1 population of cells that contained less than two sets of chromosomes was also measured. A dose dependent increase in subG1 cells was seen between 0.9 and 4 nM but decreased prior to the onset of G2/M arrest. The increase in the subG1 population did not correlate with increase in toxicity, and images of cells that were included in this population by the image analysis algorithm clearly show a population of smaller cells rather than debris (see the Supporting Information).

Micronuclei form when chromosome fragments or whole chromosomes remain in the cytoplasm after cell division and can be induced by chemicals that cause DNA strand breaks or disrupt the mitotic apparatus, respectively.<sup>59,60</sup> **1** induced micronuclei starting at 8 nM in a dose-dependent manner (Figure 3). Micronuclei began to decrease above 79 nM due to massive cell cycle arrest. This prevented progression through mitosis, which is necessary for expression of micronuclei.

Centrosome amplification occurs when the centrosome duplication cycle is uncoupled during S phase and duplication continues during mitotic delay.<sup>61</sup> The amplification of centrosomes has been shown to occur in response to antimicrotubule drugs and serves as an additional marker of tubulin disruption.<sup>62</sup> Results depicted in Figure 4 show that **1** caused a slight dose-dependent decrease in centrosome amplification up to 4 nM with a maximum decrease of approximately 2-fold compared to the negative control. Starting at 8 nM, **1** caused a steep dose-dependent increase in centrosome amplification with a maximum increase of

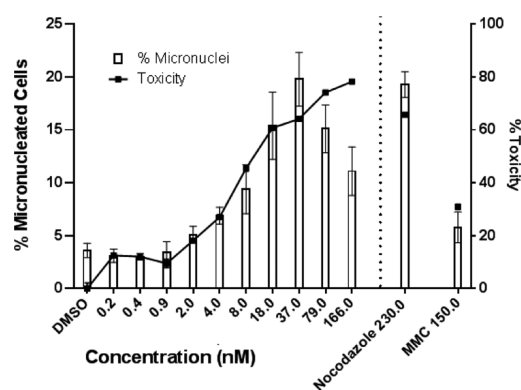


**Figure 3.** Micronucleus induction after treatment with **1** for 24 h. Percent micronucleated cells (white bars) and toxicity (solid line).

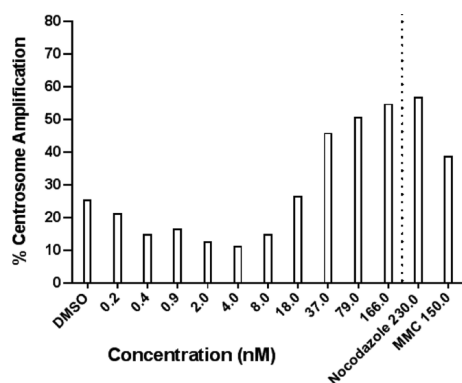


**Figure 4.** Centrosome amplification after treatment with **1** for 24 h; for each concentration, the % of cells containing >2 centrosomes was calculated.

approximately 2-fold above the negative control. The maximum increase is comparable to the response with the positive control nocodazole and represents a potent response.

An antibody specific to  $\alpha$ -tubulin was used for immunofluorescence imaging of tubulin effects after treatment with **1**. Figure 5 shows that **1** induced a drastic change in tubulin morphology, which includes tubulin condensation. The lowest dose leading to visible microtubule disruption was 8 nM.

After 24 h of exposure in U2OS cells, **1** induces micronuclei, centrosome amplification, tubulin disruption and cell cycle arrest consistent with a tubulin poison. At low concentrations, those below any observable toxicity in the investigated cell line and in the range of 0.9–4 nM, leiodermatolide causes an accumulation of cells that have less than 2N DNA content. The 0.9–4 nM concentration range also causes a decrease in the number of centrosome amplified cells compared to control. Together, these data suggest that cell cultures treated with **1** are being arrested at a point prior to S phase but after completion of mitosis, and that mitosis in the presence of this compound causes hypodiploidy. Examination of the images used in the analysis confirms that the cells being identified as having less than 2N DNA content are indeed small cells rather than debris.

Starting at 8 nM, **1** induced an increase in micronuclei, centrosome amplification and G2/M cell cycle arrest when compared to the control cultures treated with the solvent DMSO. Additionally, the 8 nM treatment concentration was the first dose that led to observations of changes in tubulin morphology. The cellular effects observed with low/nontoxic concentrations of **1** have not been reported previously for tubulin poisons. However, the cellular effects observed starting at 8 nM **1** are consistent with other tubulin poisons such as nocodazole, noscapine, colchicine and vinblastine. Noteworthy is that in cell free assays no tubulin binding could be observed. In particular, neither the tubulin polymerization assay nor other biophysical assays including SEC-LCMS, tubulin-tryptophan quenching and isothermal titration calorimetry (ITC) could provide any evidence for direct tubulin binding (data not shown). Since **1** causes centrosome effects at subtoxic concentrations that preceded tubulin disruption, a potential

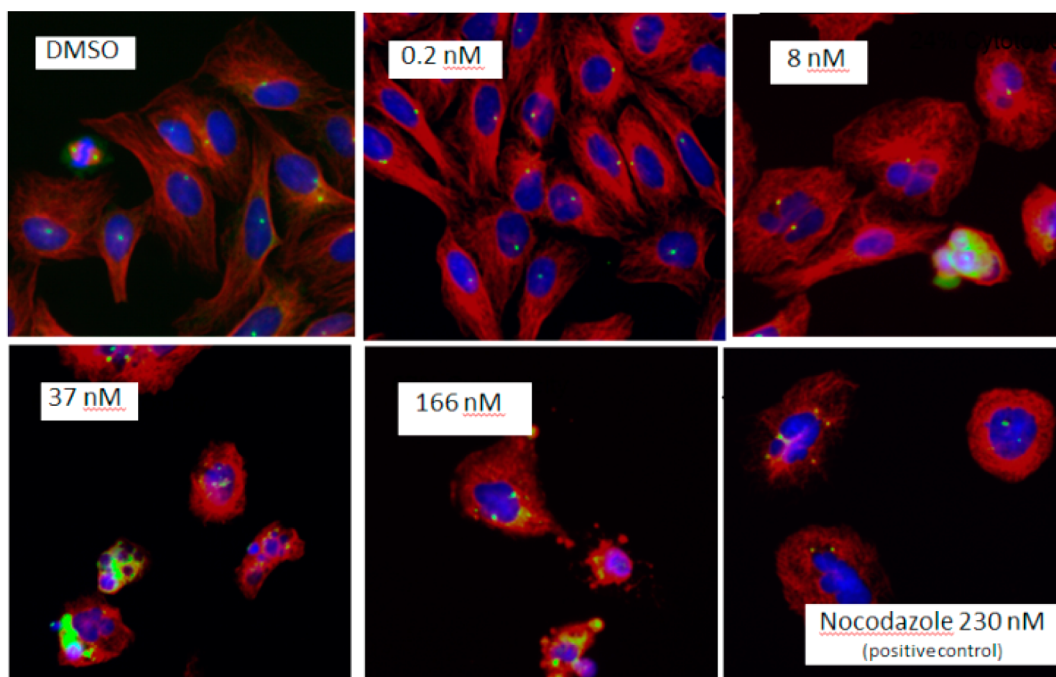


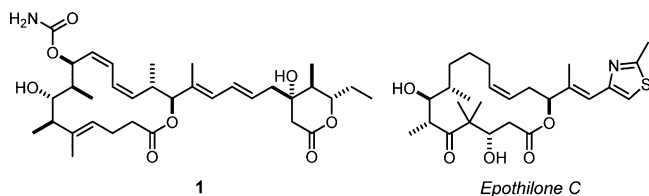
**Figure 5.** Tubulin disruption: Images of cells treated with **1** for 24 h ( $\alpha$ -tubulin: red, nuclei: blue, centrosomes: green dots).

mechanism of action is centrosome declustering. A recent study of centrosome declustering drugs shows a similar pattern of mitotic arrest followed by a peak in the subG1 (hypodiploid) cell population at the 24 h time point.<sup>63</sup> Further studies to understand centrosome toxicity will include a measure of centrosome declustering by staining for both  $\gamma$ -tubulin and centrin-2. Additionally, signal cascades related to centrosome-influenced cell cycle checkpoints (phosphorylation of TACC3) could serve as a measurement of centrosome disruption in the subG1 cell population.<sup>64</sup>

To elucidate alternative biological targets for **1**, a broad panel kinase screen was performed. No significant inhibition was observed at 1  $\mu$ M compound concentration for any of the investigated 50 representative kinases (see the Supporting Information).

## CONCLUSIONS

It was only by total synthesis that the stereostructure of leiodermatolide (**1**) could be defined; the original route that had solved this puzzle has now been revised such that a meaningful supply of this scarce cytotoxin is secured. Moreover, deliberate digression from the successful synthesis path brought a first set of analogues into reach that allowed the possible lead qualities of **1** to be assessed. In fact, **1** and its synthetic congeners **45** and **42** turned out to be exquisitely potent vis-à-vis a panel of human cancer cell lines, including a leukemia cell line expressing the Pgp efflux transporter. The acquired biological data confirm that **1** causes spindle dysfunction and mitotic arrest, yet does not bind to purified tubulin directly in a cell-free assay; its mode of action is therefore distinctly different from that of clinically approved tubulin-binding drugs. We like to emphasize this fact as one may be tempted to see a certain structural resemblance between **1** and the prominent spindle poisons of the epothilone family when the structures are drawn as shown.



Although spindle disruption cannot be entirely ruled out as a mechanism of action, indirect evidence suggests that leiodermatolide acts by centrosome declustering. If confirmed in future studies, this mode of action might be a valuable trait in that healthy adult human cells do not exhibit centrosome amplification and are therefore inherently less sensitive to centrosome declustering agents than malignant tissue.<sup>63</sup>

## ASSOCIATED CONTENT

### Supporting Information

Experimental part including characterization data, copies of NMR spectra of new compounds, supporting crystallographic information and description of the biological methods. This material is available free of charge via the Internet at <http://pubs.acs.org>.

## AUTHOR INFORMATION

**Corresponding Author**  
fuerstner@kofo.mpg.de

## Notes

The authors declare the following competing financial interest(s): Patent application submitted.

## ACKNOWLEDGMENTS

Generous financial support by the MPG and the Fonds der Chemischen Industrie (Kekulé stipend for J. W.) is gratefully acknowledged. We thank Mr. J. Rust and Prof. C. W. Lehmann for solving the X-ray structures, and the analytical departments of the MPI for excellent support. We also thank Xingzhi Tan and Weidong Ding for conducting the tubulin polymerization and tubulin binding assays.

## REFERENCES

- (1) (a) Paterson, I.; Dalby, S. M.; Roberts, J. C.; Naylor, G. J.; Guzman, E. A.; Isbrucker, R.; Pitts, T. P.; Linley, P.; Divlianska, D.; Reed, J. K.; Wright, A. E. *Angew. Chem., Int. Ed.* **2011**, *50*, 3219–3223. (b) Wright, A. E.; Reed, J. K.; Roberts, J.; Longley, R. E. U. S. Pat. Appl. Publ. US 20080033035 A1 20080207, 2008.
- (2) *Anticancer Agents from Natural Products*; Cragg, G. M., Kingston, D. G. I., Newman, D. J., Eds.; CRC Press: Boca Raton, FL, 2005.
- (3) (a) Altmann, K.-H.; Gertsch, J. *Nat. Prod. Rep.* **2007**, *24*, 327–357. (b) Rohena, C. C.; Mooberry, S. L. *Nat. Prod. Rep.* **2014**, *31*, 335–355.
- (4) (a) Gascoigne, K. E.; Taylor, S. S. *J. Cell Sci.* **2009**, *122*, 2579–2585. (b) Dumontet, C.; Jordan, M. A. *Nat. Rev. Drug Discovery* **2010**, *9*, 790–803. (c) Kavallaris, M. *Nat. Rev. Cancer* **2010**, *10*, 1–11.
- (5) Willwacher, J.; Kausch-Busies, N.; Fürstner, A. *Angew. Chem., Int. Ed.* **2012**, *51*, 12041–12046.
- (6) Paterson, I.; Ng, K. K.-H.; Williams, S.; Millican, D. C.; Dalby, S. M. *Angew. Chem., Int. Ed.* **2014**, *53*, 2692–2995.
- (7) For studies towards leiodermatolide, see: (a) Paterson, I.; Paquet, T.; Dalby, S. M. *Org. Lett.* **2011**, *13*, 4398–4401. (b) Rink, C.; Navickas, V.; Maier, M. E. *Org. Lett.* **2011**, *13*, 2334–2337. (c) Navickas, V.; Rink, C.; Maier, M. E. *Synlett* **2011**, 191–194.
- (8) Sponge specimens collected off Ft. Lauderdale contained about 10-fold more leiodermatolide than sponges of the same genus collected in the Bahamas, see ref 1; moreover, *Leiodermatium* sponges collected off Palau had only given structurally unrelated secondary metabolites of mixed polyketide/nonribosomal peptide synthetase origin (“leiotoxides”); see: (a) Sandler, J. S.; Colin, P. L.; Kelly, M.; Fenical, W. J. *Org. Chem.* **2006**, *71*, 7245–7251; Correction: *J. Org. Chem.* **2006**, *71*, 8684. (b) Larivée, A.; Unger, J. B.; Thomas, M.; Wirtz, C.; Dubost, C.; Handa, S.; Fürstner, A. *Angew. Chem., Int. Ed.* **2011**, *50*, 304–309.
- (9) Kuttruff, C. A.; Eastgate, M. D.; Baran, P. S. *Nat. Prod. Rep.* **2014**, *31*, 419–432.
- (10) Suzuki, A. *Angew. Chem., Int. Ed.* **2011**, *50*, 6722–6737.
- (11) (a) Uenishi, J.; Beau, J.-M.; Armstrong, R. W.; Kishi, Y. *J. Am. Chem. Soc.* **1987**, *109*, 4756–4758. (b) Frank, S. A.; Chen, H.; Kunz, R. K.; Schnaderbeck, M. J.; Roush, W. R. *Org. Lett.* **2000**, *2*, 2691–2694.
- (12) The use of (1R)-**12** affords the required product **8**; unfortunately, our Communication (ref 5) erroneously features the enantiomeric reagent (1S)-**12** for the preparation of this compound.
- (13) Canales, E.; Prasad, K. G.; Soderquist, J. A. *J. Am. Chem. Soc.* **2005**, *127*, 11572–11573.
- (14) Fürstner, A. *Angew. Chem., Int. Ed.* **2013**, *52*, 2794–2819.
- (15) (a) Fürstner, A.; Seidel, G. *Angew. Chem., Int. Ed.* **1998**, *37*, 1734–1736. (b) Fürstner, A.; Davies, P. W. *Chem. Commun.* **2005**, 2307–2320.
- (16) (a) Fürstner, A.; Mathes, C.; Lehmann, C. W. *J. Am. Chem. Soc.* **1999**, *121*, 9453–9454. (b) Fürstner, A.; Mathes, C.; Lehmann, C. W. *Chem.—Eur. J.* **2001**, *7*, 5299–5317.
- (17) Heppekausen, J.; Stade, R.; Kondoh, A.; Seidel, G.; Goddard, R.; Fürstner, A. *Chem.—Eur. J.* **2012**, *18*, 10281–10299.

- (18) (a) Heppekausen, J.; Stade, R.; Goddard, R.; Fürstner, A. *J. Am. Chem. Soc.* **2010**, *132*, 11045–11057. (b) Persich, P.; Llaveria, J.; Lhermet, R.; de Haro, T.; Stade, R.; Kondoh, A.; Fürstner, A. *Chem.—Eur. J.* **2013**, *19*, 13047–13058. (c) Lhermet, R.; Fürstner, A. *Chem.—Eur. J.* **2014**, *20*, 13188–13193.
- (19) Hoover, J. M.; Steves, J. E.; Stahl, S. S. *Nat. Protoc.* **2012**, *7*, 1161–1166.
- (20) Baker, R.; Castro, J. L. *J. Chem. Soc., Perkin Trans. 1* **1990**, 47–65.
- (21) (a) Abiko, A.; Liu, J.-F.; Masamune, S. *J. Am. Chem. Soc.* **1997**, *119*, 2586–2587. (b) Inoue, T.; Liu, J.-F.; Buske, D. C.; Abiko, A. *J. Org. Chem.* **2002**, *67*, 5250–5256. (c) see also: Menche, D.; Hassfeld, J.; Li, J.; Mayer, K.; Rudolph, S. *J. Org. Chem.* **2009**, *74*, 7220–7229.
- (22) (a) Bonini, C.; Chiummiento, L.; Videtta, V. *Synlett* **2005**, 3067–3070. (b) Bonini, C.; Chiummiento, L.; Videtta, V. *Synlett* **2006**, 2079–2082.
- (23) (a) Micoine, K.; Fürstner, A. *J. Am. Chem. Soc.* **2010**, *132*, 14064–14066. (b) Micoine, K.; Persich, P.; Llaveria, J.; Lam, M.-H.; Maderna, A.; Loganzo, F.; Fürstner, A. *Chem.—Eur. J.* **2013**, *19*, 7370–7383.
- (24) Northrup, A. B.; MacMillan, D. W. C. *J. Am. Chem. Soc.* **2002**, *124*, 6798–6799.
- (25) Evans, D. A.; Ng, H. P.; Clark, J. S.; Rieger, D. L. *Tetrahedron* **1992**, *48*, 2127–2142.
- (26) Einhorn, J.; Einhorn, C.; Ratajczak, F.; Pierre, J.-L. *J. Org. Chem.* **1996**, *61*, 7452–7454.
- (27) Evans, D. A.; Chapman, K. T.; Carreira, E. M. *J. Am. Chem. Soc.* **1988**, *110*, 3560–3578.
- (28) Although we were aware that MOM-cleavage can be troublesome in the presence of acid-labile functionality, the choice of this slim protecting group was dictated by the fact that neither a TIPS nor a PMB-group could be efficiently attached to the C.7-OH at this stage.
- (29) Model studies showed that carbamate formation by monoacylation of macrocyclic C7/C9-diol derivatives results in poor selectivity and favors the undesired isomer, cf. ref 7; for a possible solution, though not high yielding, see ref 6.
- (30) Kuwajima, I.; Doi, Y. *Tetrahedron Lett.* **1972**, *12*, 1163–1166.
- (31) An alternative purely organocatalytic approach was studied but found not to be competitive with this auxiliary-based tactics. In our hands, the proline-catalyzed *anti*-aldol reaction of propionaldehyde invariably gave a modest diastereoselectivity when performed on a >1 g scale (2:1 rather than 4:1, as described in ref 24), and all attempts at converting the crude product into the corresponding methyl ester by a triazolium-catalyzed aldehyde oxidation/esterification met with poor results according to the procedure described in Brooks, E. M.; Chan, A.; Phillips, E. M.; Scheidt, K. *Tetrahedron* **2009**, *65*, 3102–3109.
- (32) Uno, B. E.; Gillis, E. P.; Burke, M. D. *Tetrahedron* **2009**, *65*, 3130–3138.
- (33) Wu, T. R.; Shen, L.; Chong, J. M. *Org. Lett.* **2004**, *6*, 2701–2704.
- (34) (a) Lou, S.; Moquist, P. N.; Schaus, S. E. *J. Am. Chem. Soc.* **2006**, *128*, 12660–12661. (b) Barnett, D. S.; Moquist, P. N.; Schaus, S. E. *Angew. Chem., Int. Ed.* **2009**, *48*, 8679–8682.
- (35) (a) Barnett, D. S.; Schaus, S. E. *Org. Lett.* **2011**, *13*, 4020–4023. (b) For a review on asymmetric ketone propargylation, see: Wisniewska, H. M.; Jarvo, E. R. *J. Org. Chem.* **2013**, *78*, 11629–11639.
- (36) However, the reaction may not be general because attempted asymmetric propargylations of ethyl or *tert*-butyl 3-oxo-butanoate led to complex mixtures.
- (37) Grayson, M. N.; Goodman, J. M. *J. Org. Chem.* **2013**, *78*, 8796–8801.
- (38) Farina, V.; Krishnamurthy, V.; Scott, W. J. *Org. React.* **1997**, *50*, 1–652.
- (39) For pertinent examples, see: (a) Gagnepain, J.; Moulin, E.; Fürstner, A. *Chem.—Eur. J.* **2011**, *17*, 6964–6972. (b) Fürstner, A.; Bouchez, L. C.; Funel, J.-A.; Liepins, V.; Porée, F.-H.; Gilmour, R.; Beauflis, F.; Laurich, D.; Tamiya, M. *Angew. Chem., Int. Ed.* **2007**, *46*, 9265–9270. (c) Fürstner, A.; Bouchez, L. C.; Morency, L.; Funel, J.-A.; Liepins, V.; Porée, F.-H.; Gilmour, R.; Laurich, D.; Beauflis, F.; Tamiya, M. *Chem.—Eur. J.* **2009**, *15*, 3983–4010.
- (40) (a) Smith, N. D.; Mancuso, J.; Lautens, M. *Chem. Rev.* **2000**, *100*, 3257–3282. (b) Trost, B. M.; Ball, Z. T. *Synthesis* **2005**, 853–887.
- (41) Nicolaou, K. C.; Jiang, X.; Lindsay-Scott, P. J.; Corbu, A.; Yamashiro, S.; Bacconi, A.; Fowler, V. M. *Angew. Chem., Int. Ed.* **2011**, *50*, 1139–1144.
- (42) For other examples, see: (a) Neuhaus, C. M.; Liniger, M.; Stieger, M.; Altmann, K.-H. *Angew. Chem., Int. Ed.* **2013**, *52*, 5866–5870. (b) Brewitz, L.; Llaveria, J.; Yada, A.; Fürstner, A. *Chem.—Eur. J.* **2013**, *19*, 4532–4537.
- (43) Model studies suggested that deiodination is as fast as or faster than alkyne semireduction.
- (44) Fürstner, A.; Funel, J.-A.; Tremblay, M.; Bouchez, L. C.; Nevado, C.; Waser, M.; Ackerstaff, J.; Stimson, C. C. *Chem. Commun.* **2008**, 2873–2875.
- (45) The individual components of this system had previously been used separately, cf.: (a) Allred, G. D.; Liebeskind, L. S. *J. Am. Chem. Soc.* **1996**, *118*, 2748–2749. (b) Srogl, J.; Allred, G. D.; Liebeskind, L. S. *J. Am. Chem. Soc.* **1997**, *119*, 12376–12377.
- (46) These conditions have been widely used by us and others in advanced syntheses; for pertinent applications, see refs 6, 7a, b, 8b, 39, 52b, 56 and the following: (a) Fürstner, A.; Ackerstaff, J. *Chem. Commun.* **2008**, 2870–2872. (b) Francais, A.; Leyva, A.; Etxebarria-Jardi, G.; Ley, S. V. *Org. Lett.* **2010**, *12*, 340–343. (c) Paley, R. S.; Berry, K. E.; Liu, J. M.; Sanan, T. T. *J. Org. Chem.* **2009**, *74*, 1611–1620. (d) Paterson, I.; Kan, S. B. J.; Gibson, L. J. *Org. Lett.* **2010**, *12*, 3724–3727. (e) Paterson, I.; Gibson, L. J.; Kan, S. B. J. *Org. Lett.* **2010**, *12*, 5530–5533. (f) Otero, L.; Vaz, B.; Alvarez, R.; de Lera, A. R. *Chem. Commun.* **2013**, 49, 5043–5045. (g) Dominguez, M.; Alvarez, S.; Alvarez, R.; de Lera, A. R. *Tetrahedron* **2012**, *68*, 1756–1761. (h) Müller, S.; Mayer, T.; Sasse, F.; Maier, M. E. *Org. Lett.* **2011**, *13*, 3940–3943. (i) Paley, R. S.; Laupheimer, M. C.; Erskine, N. A. K.; Rablen, P. R.; Pike, R. D.; Jones, J. S. *Org. Lett.* **2011**, *13*, 58–61. (j) Francais, A.; Leyva-Pérez, A.; Etxebarria-Jardi, G.; Pena, J.; Ley, S. V. *Chem.—Eur. J.* **2011**, *17*, 329–343. (k) Renata, H.; Zhou, Q.; Baran, P. S. *Science* **2013**, *339*, 59–63.
- (47) Boland, W.; Schroer, N.; Sieler, C.; Feigel, M. *Helv. Chim. Acta* **1987**, *70*, 1025–1040.
- (48) For other instructive cases, see: (a) Hickmann, V.; Kondoh, A.; Gabor, B.; Alcarazo, M.; Fürstner, A. *J. Am. Chem. Soc.* **2011**, *133*, 13471–13480. (b) Chaladaj, W.; Corbet, M.; Fürstner, A. *Angew. Chem., Int. Ed.* **2012**, *51*, 6929–6933. (c) Hoffmeister, L.; Persich, P.; Fürstner, A. *Chem.—Eur. J.* **2014**, *20*, 4396–4402. (d) Willwacher, J.; Fürstner, A. *Angew. Chem., Int. Ed.* **2014**, *53*, 4217–4221. (e) Guy, A.; Oger, C.; Heppekausen, J.; Signorini, C.; De Felice, C.; Fürstner, A.; Durand, T.; Galano, J.-M. *Chem.—Eur. J.* **2014**, *20*, 6374–6380.
- (49) Fürstner, A. *Science* **2013**, *341*, 1229713.
- (50) 11/CH<sub>2</sub>Cl<sub>2</sub> is known to be incompatible with free alcohols, see ref 16.
- (51) Schrock, R. R. *Chem. Rev.* **2002**, *102*, 145–179.
- (52) (a) Gebauer, K.; Fürstner, A. *Angew. Chem., Int. Ed.* **2014**, *53*, 6393–6396. (b) Valot, G.; Regens, C. S.; O'Malley, D. P.; Godineau, E.; Takikawa, H.; Fürstner, A. *Angew. Chem., Int. Ed.* **2013**, *52*, 9534–9538.
- (53) Kočovský, P. *Tetrahedron Lett.* **1986**, *27*, 5521–5524.
- (54) (a) Guindon, Y.; Morris, H. E.; Yoakim, C. *Tetrahedron Lett.* **1983**, *24*, 3969–3972. (b) Guindon, Y.; Yoakim, C.; Morton, H. E. *J. Org. Chem.* **1984**, *49*, 3912–3920.
- (55) (a) Wilson, R. M.; Danishefsky, S. J. *J. Org. Chem.* **2006**, *71*, 8329–8351. (b) Wilson, R. M.; Danishefsky, S. J. *Angew. Chem., Int. Ed.* **2010**, *49*, 6032–6056. (c) Szpilman, A. M.; Carreira, E. M. *Angew. Chem., Int. Ed.* **2010**, *49*, 9592–9628. (d) Fürstner, A. *Isr. J. Chem.* **2011**, *51*, 329–345. (e) Wach, J.-Y.; Gademann, K. *Synlett* **2012**, 23, 163–170.
- (56) This conformational detail is reminiscent of the solution structure of iejimalide B, in which an *E,E*-configured 1,3-diene also forms a “wall” perpendicular to the plane of the macrocycle of this

exceptionally potent cytotoxic agent; this substructure is an integral part of the pharmacophore; see: (a) Gagnepain, J.; Moulin, E.; Nevado, C.; Waser, M.; Maier, A.; Kelter, G.; Fiebig, H.-H.; Fürstner, A. *Chem.—Eur. J.* **2011**, *17*, 6973–6984. (b) Moulin, E.; Nevado, C.; Gagnepain, J.; Kelter, G.; Fiebig, H.-H.; Fürstner, A. *Tetrahedron* **2010**, *66*, 6421–6428.

(57) Chari, R. V. J.; Miller, M. L.; Widdison, W. C. *Angew. Chem., Int. Ed.* **2014**, *53*, 3796–3827.

(58) Heard, P. L.; Rubitski, E. E.; Spellman, R. A.; Schuler, M. J. *Environ. Mol. Mutagen.* **2013**, *54*, 308–316.

(59) Kirsch-Volders, M. *Mutat. Res.* **1997**, *392*, 1–4.

(60) Parry, J. M.; Sors, A. *Mutat. Res.* **1993**, *287*, 3–15.

(61) Meraldi, P.; Nigg, E. A. *FEBS Lett.* **2002**, *521*, 9–13.

(62) Karna, P.; Rida, P. C.; Pannu, V.; Gupta, K. K.; Dalton, W. B.; Joshi, H.; Yang, V. W.; Zhou, J.; Aneja, R. *Cell Death Differ.* **2011**, *18*, 632–644.

(63) Ogden, A.; Cheng, A.; Rida, P. C. G.; Pannu, V.; Osan, R.; Clewley, R.; Aneja, R. *Cell Death Dis.* **2014**, *5*, e1204.

(64) Schmidt, S.; Schneider, L.; Essmann, F.; Cirstea, I. C.; Kuck, F.; Kletke, A.; Jänicke, R. U.; Wiek, C.; Hanenberg, H.; Ahmadian, M. R.; Schulze-Osthoff, K.; Nürnberg, B.; Piekorz, R. P. *Oncogene* **2010**, *29*, 6184–6192.